

Concave Comparison Functions for Accelerating Constrained Lyapunov Decay

Shuyuan Fan, Guanru Pan, and Herbert Werner

Abstract—What limits how fast a Lyapunov function can decay under input bounds? We address this question by showing how the *shape* of Lyapunov comparison functions governs guaranteed decay for control-affine systems. Using a windowed nominal exponential rate together with the endpoint cap induced by actuator limits, we establish a strict ordering: concave comparison functions strictly outperform linear and convex ones, and strict concavity is necessary to improve the best achievable global exponential rate under a fixed endpoint cap. We derive a computable lower bound on the required actuation level for a target nominal rate and show that only concave shaping can reduce this level under the endpoint cap. We then establish a feasibility-preserving acceleration result: whenever a margin exists on a sublevel set, a feasible linear comparison can be replaced by a concave one that preserves feasibility while strictly increasing the guaranteed windowed decay. Finally, we give a tunable rational concave factor with controlled slope that yields a constructive design and integrates with CLF–QP, as illustrated by examples.

Index Terms—Lyapunov methods, concave comparison functions, input saturation, CLF–QP

I. INTRODUCTION

Safety-critical systems (e.g., robotics, automotive, power, and aerospace systems) routinely operate under hard actuator bounds. These bounds cap the certified Lyapunov decay rate and thus the guaranteed settling time. This paper asks: *What fundamentally limits Lyapunov decay under input bounds, and how should the comparison function be shaped to exploit available actuation most effectively?*

A. Comparison principle

The comparison principle is a cornerstone of Lyapunov analysis for nonlinear systems. In its basic form (e.g., [1, Lem. 4.4], [2, Secs. 3.4, 4.4], and [3, App. A]), if a smooth positive-definite $V : \mathbb{R}^n \rightarrow \mathbb{R}_{\geq 0}$ satisfies

$$\dot{V}(x) \leq -\alpha(V(x)), \quad (1)$$

for some class- \mathcal{K} function $\alpha : \mathbb{R}_{\geq 0} \rightarrow \mathbb{R}_{\geq 0}$ (cf. the *comparison function* or *Lyapunov decay rate*), then we obtain the *comparison scalar ODE* (upper-bound system):

$$\dot{y} = -\alpha(y), \quad y(0) = V(x_0), \quad (2)$$

The authors are with the Institute of Control Systems, Hamburg University of Technology, Harburger Schloßstraße 22a, 21079 Hamburg, Germany (e-mail: shuyuan.fan@tuhh.de; guanru.pan@tuhh.de; h.werner@tuhh.de)

which provides a class- \mathcal{KL} estimate that

$$\dot{V}(x(t)) \leq \beta(y_0, t), \quad \forall t \geq 0. \quad (3)$$

where $\beta(y_0, t)$ is the solution of (2). Thus, the upper-bound system (2) yields a rigorous worst-case decay bound on $V(x(t))$ for estimation and analysis.

B. Background and Motivation

Beyond analysis, comparison functions play a constructive role in the control Lyapunov function (CLF) based control. In the CLF framework, originating with Artstein [4] and made explicit by Sontag's universal formula [5], the decay constraint $\dot{V}(x, u) \leq -\alpha(V)$ (cf. inequality (7)) is enforced as a design condition to certify stabilizability and parameterize the admissible feedback set. In practice, three types of comparison functions are mainly considered: (i) the *linear* comparison $\alpha(V) = \sigma V$ yielding exponential decay with rate σ , (ii) the *root* comparison $\alpha(V) = CV^p$ with $C > 0$ and $p \in (0, 1)$ guaranteeing finite-time convergence (see [6]), and (iii) *polynomial* mixtures such as $\alpha(V) = C_1 V^p + C_2 V^q$ with $0 < p < 1 < q$, invoked for fixed-time convergence (see [7]).

The latter two are non-Lipschitz at the origin and are rarely used in optimization-based control because they complicate KKT regularity and state-control mappings [8]. In addition, the over-aggressive decay around the origin, induced by the non-Lipschitz properties, contradicts the well-posedness theorem (cf. [2, Thm 3.1]) and causes chattering (see [9]). Consequently, the linear type $\alpha(V) = \sigma V$ has become the default performance constraint in many CLF-driven designs, e.g., CLF/CBF–QP (see [10]–[13]), control contraction metrics based optimal control (see [14]), and LMI control formulations (see [15]), with the exponential rate σ serving as the performance metric.

In a constrained CLF setting [16]–[18], actuator limits impose level-wise caps on admissible Lyapunov decay, thereby constraining feasible CLFs and their decay rates. From the CLF–QP perspective with a linear comparison $\alpha(V) = \sigma V$, feasibility under input limits is typically maintained by either (i) reducing σ (conservative), or (ii) introducing a penalized slack $\delta \geq 0$ in the QP, which relaxes the constraint and thus weakens the certified decay. With the linear comparison, σ becomes the sole performance objective; acceleration strategies therefore either *schedule* it (e.g., rapidly exponentially stabilizing CLF–QP [19]) or *optimize* it online as a decision variable (e.g., flexible ES–CLF–QP [20] and optimal-decay CLF–QP [21]). This single-rate reliance limits design flexibility for decay shaping under actuator saturation.

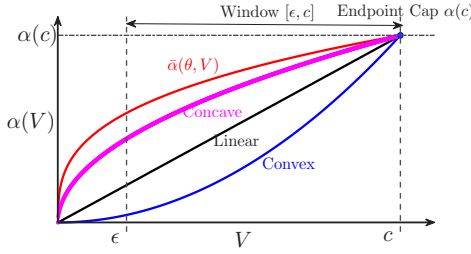


Fig. 1. Sketch: decay cap, endpoint cap, evaluation window $[\epsilon, c]$. The concave curve lies above linear and convex comparison, hence the largest $\sigma_\alpha(\epsilon, c)$ is guaranteed.

Rather than only scaling the rate (increasing σ), we ask a complementary question: How does the *shape* of α (linear, convex, concave, or mixtures) mediate the trade-off between feasibility and guaranteed decay under fixed input bounds? Figure 1 gives a quick visual: under a common endpoint cap $\alpha(c)$, a strictly concave α lies above the linear and convex ones on $(0, c)$ and thus certifies a larger guaranteed decay (equivalently, a larger windowed nominal rate $\sigma_\alpha(\epsilon, c)$).

C. Contributions

We develop a shape-aware framework for Lyapunov decay under input saturation, evaluated through windowed performance metrics. Our main contributions are:

- **Decay acceleration by the concave comparison.** For the upper-bound ODE (2), on any window $[\epsilon, c]$ and under a common endpoint cap, strictly concave comparisons guarantee a strictly larger windowed nominal rate $\sigma_\alpha(\epsilon, c)$ than linear or convex ones. Moreover, any improvement over the linear baseline with the same endpoint cap requires *strict* concavity on a nontrivial subset of $(0, c)$.
- **Lower peak actuation for higher certified rate.** We derive the actuation level required to achieve a target windowed rate and show that, under a linear comparison, higher nominal rates demand higher (endpoint-dominated) actuation level. In contrast, concave shaping achieves a strictly larger $\sigma_\alpha(\epsilon, c)$ with a smaller actuation level.
- **Feasibility-preserving acceleration.** Whenever a margin exists on a sublevel set, a feasible linear comparison can be replaced by a concave one that preserves feasibility while increasing the guaranteed decay over the window.
- **Constructive concave design.** We introduce a Lipschitz rational concave factor with closed-form normalization and slope control, enabling practical tuning and integration with CLF-QP.

Notation

\mathbb{R} , $\mathbb{R}_{\geq 0}$, and $\mathbb{R}_{> 0}$ denote the real, nonnegative real, and positive real numbers. For $x \in \mathbb{R}^n$, $\|x\|$ is the Euclidean norm, $\|x\|_1 = \sum_{i=1}^n |x_i|$, and $\|x\|_\infty = \max_i |x_i|$. For a matrix A , A^\top is its transpose; $\text{diag}(\cdot)$ builds a diagonal matrix; $A \succ 0$ ($A \prec 0$) means positive (negative) definite. For $A \succ 0$, $\lambda_{\min}(A)$ and $\lambda_{\max}(A)$ denote its smallest and largest eigenvalues. All functions are locally Lipschitz unless stated

otherwise; C^k denotes k -times continuously differentiable. For $f : \mathbb{R} \rightarrow \mathbb{R}$, $f'(x) = \frac{df}{dx}$. For $f : \mathbb{R}^n \rightarrow \mathbb{R}$, the gradient is $\nabla f(x) = [\partial f/\partial x_1, \dots, \partial f/\partial x_n]^\top$. Time derivatives are denoted by a dot, e.g., \dot{x} . Lie derivatives $L_f V := \nabla V^\top f$, $L_g V := \nabla V^\top g$. $\alpha \in \mathcal{K}$ means $\alpha : [0, a) \rightarrow [0, \infty)$ is continuous, $\alpha(0) = 0$, and strictly increasing on $[0, a)$. $\alpha \in \mathcal{K}_{\text{vex}}/\mathcal{K}_{\text{cave}}/\mathcal{K}_l$ implies $\alpha \in \mathcal{K}$ and α is strictly convex/strictly concave/linear, respectively.

II. PRELIMINARIES

We consider the control-affine system

$$\dot{x} = f(x) + g(x)u, \quad (4)$$

with $x \in \mathbb{X} \subset \mathbb{R}^n$ and $u \in \mathbb{U}(\theta) \subset \mathbb{R}^m$, where $f : \mathbb{X} \rightarrow \mathbb{R}^n$ and $g : \mathbb{X} \rightarrow \mathbb{R}^{n \times m}$ are locally Lipschitz with $f(0) = 0$ and with $g(0) \neq 0$. Inputs are bounded in:

$$\mathbb{U}(\theta) \doteq \{u \in \mathbb{R}^m \mid \|u\|_\infty \leq \theta\} \quad (5)$$

where $\theta > 0$ represents the *actuation level*. For an initial condition $x(0) = x_0$ and an admissible input $u(\cdot) \in \mathbb{U}(\theta)$ (measurable, essentially bounded), let $\phi(t, x_0, u)$ denote the Carathéodory solution of (4). We assume \mathbb{X} is compact, contains the origin, and is *control-invariant* with respect to $\mathbb{U}(\theta)$; i.e., for every $x_0 \in \mathbb{X}$ there exists an input $u(\cdot) \in \mathbb{U}(\theta)$ such that $\phi(t, x_0, u) \in \mathbb{X}$ for all $t \geq 0$.

A. Control Lyapunov functions and comparison

We begin with a standard CLF definition.

Definition 1 (Control Lyapunov function): A smooth, positive-definite $V : \mathbb{R}^n \rightarrow \mathbb{R}_{\geq 0}$ is a CLF for (4) on \mathbb{X} with inputs in $\mathbb{U}(\theta)$ if there exist $0 < k_1 \leq k_2$ and a class- \mathcal{K} function α such that, for all $x \in \mathbb{X}$,

$$k_1\|x\|^2 \leq V(x) \leq k_2\|x\|^2, \quad (6a)$$

$$\inf_{u \in \mathbb{U}(\theta)} \{L_f V(x) + L_g V(x)u + \alpha(V(x))\} \leq 0. \quad (6b)$$

The corresponding admissible feedback set (same as [19])

$$K(x) \doteq \{u \in \mathbb{U}(\theta) : L_f V(x) + L_g V(x)u \leq -\alpha(V(x))\}$$

is nonempty for all $x \in \mathbb{X}$ by (6b). Any (measurable) selection $u(x) \in K(x)$ enforces the differential inequality

$$\dot{V}(x, u) \doteq L_f V(x) + L_g V(x)u \leq -\alpha(V(x)), \quad (7)$$

which aligns with (1) and yields the scalar comparison bound $V(x(t)) \leq y(t)$, where $y(t)$ solves (2).

Linear comparison (exponential stabilizing CLF): If (6) holds with the linear comparison $\alpha(V) = \sigma V$ ($\sigma > 0$), then for any $u(x) \in K(x)$ the closed-loop system

$$\dot{x} = f(x) + g(x)u(x) \quad (8)$$

has the solution $x(t)$ satisfying the explicit estimate

$$\|x(t)\| \leq \sqrt{\frac{k_2}{k_1}} e^{-\frac{\sigma}{2}t} \|x(0)\|, \quad \forall t \geq 0, \quad (9)$$

i.e., global exponential convergence with rate $\sigma/2$. Thus, larger σ yields faster state convergence, linking the Lyapunov decay enforced by (7) to state bounds via the comparison framework (1)-(3).

B. Windowed decay metrics

Consider $0 < \epsilon < c \leq c_{\max}$ and define the sublevel set

$$\Omega(V, c) \doteq \{x : V(x) \leq c\}, \quad c_{\max} \doteq \sup\{v : \Omega(V, v) \subseteq \mathbb{X}\}.$$

Given an evaluation window $[\epsilon, c]$, we introduce windowed decay metrics for evaluating performance on this window.

Definition 2 (Nominal rate): Let the *crossing time* $T(\epsilon, c)$ be the first time at which the trajectory $V(\phi(t, x_0, u))$, initialized on the level set $V(x_0) = c$, enters $\Omega(V, \epsilon)$. The associated *nominal exponential decay rate (simply nominal rate)* over the window is

$$\sigma_{\text{nom}}(\epsilon, c) \doteq \frac{\ln(c/\epsilon)}{T(\epsilon, c)}. \quad (10)$$

For the comparison system (2) with $\alpha \in \mathcal{K}$, let $T_\alpha(\epsilon, c)$ denote the crossing time of its solution $y(t)$ with $y(0) = c$. By the chain rule, we obtain

$$T_\alpha(\epsilon, c) = \int_\epsilon^c \frac{1}{\alpha(y)} dy. \quad (11)$$

Define its windowed *nominal rate*

$$\sigma_\alpha(\epsilon, c) \doteq \frac{\ln(c/\epsilon)}{T_\alpha(\epsilon, c)}. \quad (12)$$

By the comparison principle (1)–(2) (which yields $V(x(t)) \leq y(t)$ for all $t \geq 0$), the comparison trajectory reaches ϵ no earlier than the true trajectory:

$$T_\alpha(\epsilon, c) \geq T(\epsilon, c) \iff \sigma_\alpha(\epsilon, c) \leq \sigma_{\text{nom}}(\epsilon, c). \quad (13)$$

Thus, $\sigma_\alpha(\epsilon, c)$ is a *conservative* (certified) estimate of the true nominal rate on $[\epsilon, c]$.

Linear case: For the linear comparison $\alpha(V) = \sigma V$,

$$T_\alpha(\epsilon, c) = \frac{1}{\sigma} \ln \frac{c}{\epsilon}, \quad \sigma_\alpha(\epsilon, c) \equiv \sigma \quad (\text{for any window } [\epsilon, c]).$$

Unlike the strictly pointwise constraint $\dot{V} \leq -\sigma V$ (constant rate at every level), the windowed metric (12) aggregates the guaranteed decay *over the window*, allowing structural reshaping of α (e.g., concavity) under a fixed endpoint cap to trade interior decay against feasibility. For each two adjacent subintervals $[\epsilon, c_0], [c_0, c]$, the relation of the related nominal rate is presented in (14b).

Lemma 1 (Composition of nominal rates): Consider $0 < \epsilon < c_0 < c$ and a class- \mathcal{K} comparison function α . Define

$$\sigma_1 \doteq \sigma_\alpha(\epsilon, c_0), \quad \sigma_2 \doteq \sigma_\alpha(c_0, c), \quad \lambda \doteq \ln(c/c_0)/\ln(c/\epsilon) \in (0, 1).$$

Then, the nominal rate on $[\epsilon, c]$ satisfies:

$$\frac{1}{\sigma_\alpha(\epsilon, c)} = \frac{1 - \lambda}{\sigma_1} + \frac{\lambda}{\sigma_2} \quad (14a)$$

$$\sigma_\alpha(\epsilon, c) = \frac{\sigma_1 \sigma_2}{\lambda \sigma_1 + (1 - \lambda) \sigma_2}. \quad (14b)$$

$$\min\{\sigma_1, \sigma_2\} \leq \sigma_\alpha(\epsilon, c) \leq \max\{\sigma_1, \sigma_2\}, \quad (14c)$$

with equality in (14c) if and only if $\sigma_1 = \sigma_2$ (since $\lambda \in (0, 1)$).

Proof: By definition, $T_\alpha(\epsilon, c) = T_\alpha(\epsilon, c_0) + T_\alpha(c_0, c)$,

$$\frac{1}{\sigma_\alpha(\epsilon, c)} = \frac{T_\alpha(\epsilon, c)}{\ln(c/\epsilon)} = \frac{T_\alpha(\epsilon, c_0)}{\ln(c/\epsilon)} + \frac{T_\alpha(c_0, c)}{\ln(c/\epsilon)} = \frac{1 - \lambda}{\sigma_1} + \frac{\lambda}{\sigma_2},$$

which is (14a); (14b) is algebraically rearranged. Since (14a) is a weighted harmonic mean of σ_1, σ_2 with weights $1 - \lambda$ and λ in $(0, 1)$, (14c) follows, with equality iff $\sigma_1 = \sigma_2$. ■

This lemma is useful for shaping the nominal rate: it allows one to maintain a desired overall rate while relaxing the decay constraint at high Lyapunov levels to preserve feasibility under input bounds.

C. Induced endpoint cap under input bounds

Consider a smooth CLF V . Define the pointwise decay cap

$$D_{\max}(x, \theta) \doteq \max_{u \in \mathbb{U}(\theta)} \{-L_f V(x) - L_g V(x) u\}. \quad (15)$$

For $\mathbb{U}(\theta) = \{u : \|u\|_\infty \leq \theta\}$, linear optimization over u gives

$$D_{\max}(x, \theta) = -L_f V(x) + \theta \|L_g V(x)\|_1. \quad (16)$$

At point x , an admissible decay $\alpha(V(x))$ should satisfy

$$\alpha(V(x)) \leq D_{\max}(x, \theta), \quad (17)$$

which represents the pointwise feasibility condition. The sublevel set $\Omega(V, v)$ induces a level-wise cap

$$\bar{\alpha}(\theta, v) \doteq \sup_{x \in \Omega(V, v)} D_{\max}(x, \theta), \quad 0 < v \leq c_{\max}. \quad (18)$$

which yields the necessary condition at level $V = v$:

$$\alpha(v) \leq \bar{\alpha}(\theta, v). \quad (19)$$

Since $\Omega(V, v) \subseteq \Omega(V, c)$ for $v \leq c$, $\bar{\alpha}(\theta, v) \leq \bar{\alpha}(\theta, c)$. Hence,

$$\forall 0 < V \leq c, \quad \alpha(V) \leq \alpha(c) \leq \bar{\alpha}(\theta, c).$$

Thus, under input bounds, on any window $[\epsilon, c]$ the admissible $\alpha(V)$ is capped by the *endpoint cap* $\bar{\alpha}(\theta, c)$, motivating shape design of α under a fixed endpoint.

Global exponential rate: For the linear comparison $\alpha(V) = \sigma V$, the endpoint condition $\alpha(c) = \sigma c \leq \bar{\alpha}(\theta, c)$ gives

$$\sigma \leq \bar{\alpha}(\theta, c)/c \doteq \sigma_c.$$

Actuator limits therefore impose an endpoint cap on the achievable global exponential rate. Any $\sigma > \sigma_c$ violates the necessary cap at $V = c$ for which the decay inequality is infeasible. Consequently, uniform feasibility over $\Omega(V, c)$ cannot be guaranteed.

D. Comparison functions

We mainly focus on class- \mathcal{K} comparison functions. According to shape, we classify $\alpha \in \mathcal{K}$ into four classes: linear \mathcal{K}_l , strictly concave $\mathcal{K}_{\text{cave}}$, strictly convex \mathcal{K}_{vex} , and mixed

$$\mathcal{K}_{\text{mix}} \doteq \mathcal{K} \setminus (\mathcal{K}_l \cup \mathcal{K}_{\text{cave}} \cup \mathcal{K}_{\text{vex}}).$$

Note that any $\alpha \in \mathcal{K}$ admits a quasi-linear representation:

$$\alpha(y) = s(y)y \quad (20)$$

where $s : \mathbb{R}_{\geq 0} \rightarrow \mathbb{R}_{>0}$ denotes the dynamic (scaling) factor defined as:

$$s(y) \doteq \begin{cases} \frac{\alpha(y)}{y}, & y > 0, \\ \lim_{y \rightarrow 0^+} \frac{\alpha(y)}{y} \in [0, \infty], & y = 0. \end{cases} \quad (21)$$

Here we leverage the monotonic properties of the dynamic factor about the shape of α .

Lemma 2 (Dynamic-factor characterization): Suppose $\alpha \in \mathcal{K}$ with dynamic factor s . The following statements hold:

- 1) $s(y)$ is a constant if $\alpha \in \mathcal{K}_l$;
- 2) $s(y)$ is strictly decreasing in y if $\alpha \in \mathcal{K}_{cave}$;
- 3) $s(y)$ is strictly increasing in y if $\alpha \in \mathcal{K}_{vex}$.

Proof: The linear case is obvious. By the definition of strictly concave, for $0 < \lambda < 1$ and $y > 0$, we have

$$\alpha(\lambda y + (1 - \lambda)0) > \lambda\alpha(\lambda y) + (1 - \lambda)\alpha(0)$$

which implies $s(\lambda y) > s(y)$ such that $s(y)$ is decreasing. Similarly, we can prove if $\alpha(y)$ is convex, $s(y)$ is increasing. \blacksquare

These properties will be used for analysis and construction.

Definition 3 (Concave Factor): For $\alpha \in \mathcal{K}_{cave}$, the associated s in (20) is called a concave factor that concavifies y .

The concave factor serves as a practical design handle for constructing Lipschitz class- \mathcal{K}_{cave} comparison functions.

III. CONCAVE COMPARISON FUNCTIONS FOR CONSTRAINED UPPER-BOUND DECAY

This section quantifies how the *shape* (concave, linear, convex) of a class- \mathcal{K} comparison function α governs the decay of the upper-bound system (2) on the evaluation window $[\epsilon, c]$, subject to the endpoint cap $\alpha(c) \leq \bar{\alpha}(\theta, c)$. Unless stated otherwise, “concave” and “convex” mean strictly concave/convex.

A. Decay ordering and acceleration

We mainly compare three classes \mathcal{K}_l , \mathcal{K}_{cave} , and \mathcal{K}_{vex} under the same endpoint value $\alpha(c)$, and claim that \mathcal{K}_{mix} functions lie in between. As a reminder, a class- \mathcal{K} function is continuous, strictly increasing, and satisfies $\alpha(0) = 0$; hence it is locally Lipschitz on $[\epsilon, c]$. We write $\alpha_l(y) = \sigma y \in \mathcal{K}_l$, $\alpha_{cave} \in \mathcal{K}_{cave}$, and $\alpha_{vex} \in \mathcal{K}_{vex}$.

Proposition 1 (Ordering under equal endpoint cap): Let $\alpha_l(c) = \alpha_{cave}(c) = \alpha_{vex}(c)$. Then for any $\epsilon \in (0, c)$,

$$\sigma_{\alpha_{vex}}(\epsilon, c) < \sigma_{\alpha_l}(\epsilon, c) = \frac{\alpha_l(c)}{c} < \sigma_{\alpha_{cave}}(\epsilon, c),$$

where $\sigma_{\alpha_l}(\epsilon, c)$ denote the nominal rate defined in (12).

Proof: Let s_l, s_{cave}, s_{vex} be the dynamic factors as defined in (21) of $\alpha_l, \alpha_{cave}, \alpha_{vex}$, respectively. Then, $s_{cave}(c) > s_l(c) > s_{vex}(c)$. By Lem.2, for $y \in [\epsilon, c]$, $s_{cave}(y) > s_l(y) > s_{vex}(y)$, such that $T_{\alpha_{cave}}(\epsilon, c) < T_{\alpha_l}(\epsilon, c) < T_{\alpha_{vex}}(\epsilon, c)$. Equivalently, we have $\sigma_{\alpha_{vex}}(\epsilon, c) < \sigma_{\alpha_l}(\epsilon, c) < \sigma_{\alpha_{cave}}(\epsilon, c)$. \blacksquare

Figure 1 depicts the equal-endpoint case at $y = c$. By geometry, a strictly concave α_{cave} lies above its chord while a strictly convex α_{vex} lies below; hence, for all $y \in (0, c)$,

$$\alpha_{cave}(y) > \alpha_l(y) > \alpha_{vex}(y),$$

which supports the above proposition. Moreover, concave comparisons can achieve a faster windowed decay even when the endpoint value is reduced.

Theorem 1 (Acceleration under a relaxed endpoint cap): Let $\alpha_l(y) = \sigma y$ be the linear baseline on $(0, c]$. (i) If

$\alpha_{vex} \in \mathcal{K}_{vex}$ (strictly convex) and $\alpha_{vex}(c) \leq \alpha_l(c)$, then for every $\epsilon \in (0, c)$, $\sigma_{\alpha_{vex}}(\epsilon, c) < \sigma$. (ii) Suppose $\alpha_{cave} \in \mathcal{K}_{cave}$ (strictly concave) with $\alpha_{cave}(c) < \alpha_l(c)$ and there exists $y^* \in (0, c)$ such that $\alpha_{cave}(y^*) > \alpha_l(y^*)$, then there exists $c_0 \in (y^*, c)$ and $\epsilon_0 \in (0, c_0)$ such that for all $\epsilon \in (0, \epsilon_0)$, $\sigma_{\alpha_{cave}}(\epsilon, c) > \sigma$.

Proof: Write $\alpha(y) = s(y)y$ with the dynamic factor $s(y) = \alpha(y)/y$. (i) *Convex case.* If α_{vex} is strictly convex, then s_{vex} is strictly increasing on $(0, c]$. Hence $s_{vex}(y) \leq s_{vex}(c)$ for all $y \in (0, c]$, and

$$T_{\alpha_{vex}}(\epsilon, c) = \int_{\epsilon}^c \frac{dy}{s_{vex}(y)y} \geq \frac{1}{s_{vex}(c)} \int_{\epsilon}^c \frac{dy}{y} = \frac{\ln(c/\epsilon)}{s_{vex}(c)}.$$

Since $\alpha_{vex}(c) \leq \alpha_l(c) = \sigma c$, we have $s_{vex}(c) \leq \sigma$, hence $T_{\alpha_{vex}}(\epsilon, c) \geq \frac{\ln(c/\epsilon)}{\sigma} = T_{\alpha_l}(\epsilon, c)$. Strict convexity makes the inequality strict, so $\sigma_{\alpha_{vex}}(\epsilon, c) < \sigma$. (ii) *Concave case.* If the condition holds, then $s_{cave}(y^*) > \sigma$ and $s_{cave}(c) < \sigma$. Because s_{cave} is strictly decreasing and continuous, there exists a unique $c_0 \in (y^*, c)$ with $s_{cave}(c_0) = \sigma$, i.e., $\alpha_{cave}(c_0) = \alpha_l(c_0)$. Over $(0, c_0)$ one has $s_{cave} > \sigma$, hence $\sigma_{\alpha_{cave}}(\epsilon, c_0) > \sigma$ for all $\epsilon \in (0, c_0)$; over (c_0, c) one has $s_{cave} < \sigma$, hence $\sigma_{\alpha_{cave}}(c_0, c) < \sigma$. Using the two-interval compositions (cf. (14b))

$$\sigma_{\alpha}(\epsilon, c) = \frac{\sigma_{\alpha}(\epsilon, c_0) \sigma_{\alpha}(c_0, c)}{\lambda \sigma_{\alpha}(\epsilon, c_0) + (1 - \lambda) \sigma_{\alpha}(c_0, c)}, \quad \lambda = \frac{\ln(c/c_0)}{\ln(c/\epsilon)},$$

we see that as $\epsilon \rightarrow 0$ (so $\lambda \rightarrow 0$), $\lim_{\epsilon \rightarrow 0^+} \sigma_{\alpha_{cave}}(\epsilon, c) = \sigma_{\alpha_{cave}}(0^+, c_0) > \sigma$. Using monotonicity, one can simply pick ϵ_0 with $\sigma_{\alpha_{cave}}(\epsilon_0, c) > \sigma$; then for any smaller ϵ the inequality still holds. \blacksquare

Proposition 1 and Theorem 1 together show that class- \mathcal{K}_{cave} comparison functions enable acceleration with *endpoint relaxation*: for suitable windows $[\epsilon, c]$, one can have

$$\alpha_{cave}(c) < \alpha_l(c) \quad \text{while} \quad \sigma_{\alpha_{cave}}(\epsilon, c) > \sigma = \alpha_l(c)/c.$$

Mixed shapes via window decomposition: For $\alpha_{mix} \in \mathcal{K}_{mix}$ we partition the window $[\epsilon, c]$ into subwindows

$$\epsilon = a_0 < a_1 < \dots < a_N = c,$$

on each of which α_{mix} is (i) strictly concave, (ii) linear, or (iii) strictly convex. For $y \in [a_{i-1}, a_i]$, denote the chord (secant) of α_{mix} by

$$\chi_i(y) \doteq \frac{\alpha_{mix}(a_i) - \alpha_{mix}(a_{i-1})}{a_i - a_{i-1}}(y - a_{i-1}) + \alpha_{mix}(a_{i-1}).$$

By additivity of the crossing-time integral,

$$T_{\alpha_{mix}}(\epsilon, c) = \sum_{i=1}^N \int_{a_{i-1}}^{a_i} \frac{1}{\alpha_{mix}(y)} dy.$$

On a concave subwindow, $\alpha_{mix}(y) > \chi_i(y)$ and the local integral $\int_{a_{i-1}}^{a_i} \frac{1}{\alpha_{mix}} dy$ is *reduced* relative to the chord; on a linear subwindow, $\alpha_{mix} = \chi_i$ (neutral); on a convex subwindow, $\alpha_{mix}(y) < \chi_i(y)$ and the local integral is *increased*. Consequently, only strictly concave subwindows contribute to acceleration (relative to the chord), linear subwindows are neutral, and convex subwindows degrade it.

B. Necessity of concavity under an endpoint cap

To further study comparison functions under the endpoint constraint, we introduce the following metric.

Definition 4 (Endpoint-Relaxation ratio): Define

$$r_\alpha(\epsilon, c) \doteq \frac{\alpha(c)}{\sigma_\alpha(\epsilon, c) c}, \quad 0 < \epsilon < c, \quad (22)$$

where $\sigma_\alpha(\epsilon, c)$ is defined in (12).

Interpretation: $r_\alpha(\epsilon, c) < 1$ (relaxation) reflects same rate with a *smaller* endpoint than linear, $r_\alpha = 1$ represents same rate with the *same* endpoint as linear, and $r_\alpha > 1$ means achieving the same rate requires a *larger* endpoint than linear. For the linear comparison α_l , $r_{\alpha_l} \equiv 1$ on any window.

Proposition 2 (Ordering for endpoint-relaxation ratio):

For any $[\epsilon, c] \subset (0, \infty)$, we obtain

$$r_{\alpha_{cave}}(\epsilon, c) < 1 = r_{\alpha_l}(\epsilon, c) < r_{\alpha_{vex}}(\epsilon, c)$$

whenever $\alpha_{cave} \in \mathcal{K}_{cave}$ and $\alpha_{vex} \in \mathcal{K}_{vex}$.

Proof: Linear case is immediate. For $\alpha_{cave} \in \mathcal{K}_{cave}$,

$\alpha_{cave}(y) > \alpha_{cave}(c)y/c$ holds, for all $y \in (0, c)$, which yields

$$T_{\alpha_{cave}}(\epsilon, c) < \int_\epsilon^c \frac{c dy}{\alpha_{cave}(c) y} = \frac{c}{\alpha_{cave}(c)} \ln\left(\frac{c}{\epsilon}\right).$$

Substituting it into (22), one has $r_{\alpha_{cave}} < 1$. The strictly convex case reverses the inequalities, giving $r_{\alpha_{vex}} > 1$. ■

Endpoint relaxation and concave shaping: The endpoint-relaxation ratio is *intrinsic* to a comparison function on a given window and is invariant under positive scaling: for any $k > 0$, $r_{k\alpha}(\epsilon, c) = r_\alpha(\epsilon, c)$. Hence we may take any strictly concave class- \mathcal{K} template α_{cave} and normalize/scale it to obtain a comparison function that simultaneously relaxes the endpoint and accelerates decay (cf. Sec. V).

Let the linear baseline be $\alpha_l(y) = \sigma y$ (so $\alpha_l(c) = \sigma c$), and write $\alpha_{cave}(y) = s_{cave}(y) y$ with strictly decreasing s_{cave} (the concave factor). Define

$$\alpha(y) = \frac{s_{cave}(y)}{s_{cave}(c)} r \sigma y, \quad r_{\alpha_{cave}}(\epsilon, c) < r < 1. \quad (23)$$

Then $\alpha(c) = r \sigma c$ (endpoint relaxation), and using $\sigma_{k\alpha} = k \sigma_\alpha$ together with $r > r_{\alpha_{cave}}(\epsilon, c)$ yields $\sigma_\alpha(\epsilon, c) > \sigma$, i.e., faster windowed decay with a reduced endpoint value.

Lemma 3 (Concavity is necessary for relaxation): Let $\alpha \in \mathcal{K}$ be continuous on $[0, c]$ and C^2 on $(0, c)$. If $r_\alpha(\epsilon, c) < 1$ for some $0 < \epsilon < c$, then there exists a nontrivial interval $\mathcal{I}_{cave} \subset (0, c)$ on which α is strictly concave.

Proof: Let $\chi(y) \doteq \frac{\alpha(c)}{c} y$ be the chord through $(0, 0)$ and $(c, \alpha(c))$. The condition $r_\alpha(\epsilon, c) < 1$ is equivalent to

$$T_\alpha(\epsilon, c) = \int_\epsilon^c \frac{1}{\alpha(y)} dy < \int_\epsilon^c \frac{1}{\chi(y)} dy = \frac{c}{\alpha(c)} \ln \frac{c}{\epsilon}.$$

Hence $\int_\epsilon^c \left(\frac{1}{\alpha(y)} - \frac{1}{\chi(y)} \right) dy < 0$, which implies that $\frac{1}{\alpha(y)} - \frac{1}{\chi(y)} < 0$ on a set of positive measure in (ϵ, c) . Since $\alpha, \chi > 0$ on (ϵ, c) , this yields $\alpha(y) > \chi(y)$ on such a set. Define $h(y) := \alpha(y) - \chi(y)$. Then h is continuous on $[0, c]$, C^2 on $(0, c)$, and satisfies $h(0) = h(c) = 0$ while $h > 0$ on a set of positive measure in (ϵ, c) . If $h''(y) \geq 0$ for all $y \in (0, c)$, then h would be convex, and with $h(0) = h(c) = 0$ convexity

would imply $h(y) \leq 0$ for all $y \in (0, c)$ contradicting the condition. Therefore there exists $y_0 \in (0, c)$ with $h''(y_0) < 0$. By continuity of h'' , there is a nontrivial open interval $\mathcal{I}_{cave} \ni y_0$ on which $h'' < 0$, i.e., $\alpha'' < 0$. Thus α is strictly concave on \mathcal{I}_{cave} . ■

These results show that strictly concave comparison functions (\mathcal{K}_{cave}) can *reduce the endpoint value* while still certifying *faster windowed decay*. The reduced endpoint directly lowers the required actuation level (e.g., peak input $\|u\|_\infty$), as analyzed in the next section. Moreover, for a mixed-shape comparison $\alpha \in \mathcal{K}_{mix}$, achieving endpoint relaxation on a window necessarily requires *strict concavity on a nontrivial subinterval* of $(0, c)$ (cf. Lemma 3).

IV. LYAPUNOV DECAY IN THE CLF FRAMEWORK

This section links the upper-bound decay analysis in Sec. III to the feasibility of the CLF derivative inequality (7) under input bounds. We show that the concave comparison functions reduce the lower-bound actuation level while guaranteeing faster decay.

A. Required Actuation Level for a Desired Decay

We characterize the trade-off between a target decay constraint ($\dot{V}(x, u) \leq -\alpha(V(x))$) and the required actuation level. Throughout, we make the following regular assumption.

Assumption 1 (Regularity): There exist $L_1, L_2 > 0$, and $\{\bar{g}_i\}_{i=1}^m$ such that, for all $x \in \mathbb{X}$, $\|f(x)\| \leq L_1 \|x\|$, and

$$\|\nabla V(x)\| \leq L_2 \|x\|, \quad \|g_i(x)\| \leq \bar{g}_i, \quad i = 1, \dots, m,$$

where $g(x) = [g_1(x), \dots, g_m(x)]$.

Definition 5 (Actuation level on a sublevel set): For a given $\alpha \in \mathcal{K}$ and $v > 0$, the required actuation level (minimal peak actuation $\|u\|_\infty$) to enforce $\dot{V}(x, u) \leq -\alpha(V)$ uniformly on $\Omega(V, v)$ is defined as:

$$\theta_{\min}(\alpha; v) \doteq \inf_{\theta \geq 0} \left\{ \theta : \forall x \in \Omega(V, v), \alpha(V(x)) \leq D_{\max}(x, \theta) \right\}. \quad (24)$$

Using $D_{\max}(x, \theta) = -L_f V(x) + \theta \|L_g V(x)\|_1$, (24) admits the closed form

$$\theta_{\min}(\alpha; v) = \sup_{x \in \Omega(V, v)} \left[\frac{\alpha(V(x)) + L_f V(x)}{\|L_g V(x)\|_1} \right]_+ \quad (25)$$

where $[z]_+ \doteq \max\{z, 0\}$. When $\alpha(V(x)) + L_f V(x) \leq 0$ for all $x \in \Omega(V, v)$, then $\theta_{\min}(\alpha; v) = 0$. If there exists $x \in \Omega(V, v)$ with $x \neq 0$, $\|L_g V(x)\|_1 = 0$ and $\alpha(V(x)) + L_f V(x) > 0$, then $\theta_{\min}(\alpha; v) = \infty$.

1) Small- x behavior and finiteness: We quantify when the actuation level $\theta_{\min}(\alpha; v)$ remains finite (or vanishes) as $v \rightarrow 0$. Near the origin assume, $1 \leq q_1 \leq 2$,

$$L_f V(x) = \mathcal{O}(\|x\|^2), \quad \alpha(V(x)) = \mathcal{O}(\|x\|^{q_1}),$$

and impose a *lower* growth bound on the input channel:

$$\forall \|x\| < \rho, \|L_g V(x)\|_1 \geq c_g \|x\|^{q_2}, \quad c_g > 0, \quad q_2 \geq 1. \quad (26)$$

From (25), the numerator is $\mathcal{O}(\|x\|^{\min\{q_1, 2\}}) = \mathcal{O}(\|x\|^{q_1})$, and by (26) the denominator is $\mathcal{O}(\|x\|^{q_2})$. Therefore

$$\left[\frac{\alpha(V(x)) + L_f V(x)}{\|L_g V(x)\|_1} \right]_+ = \mathcal{O}(\|x\|^{q_1 - q_2})_+,$$

and we obtain the following situations as $v \rightarrow 0$:

- **Vanishing level** if $q_2 < q_1$: $q_1 - q_2 > 0$ and $\lim_{v \rightarrow 0} \theta_{\min}(\alpha; v) = 0$.
- **Finite, nonzero limit (or bounded)** if $q_2 = q_1$: the ratio remains bounded (approaches a constant determined by leading coefficients).
- **Blow-up** if $q_2 > q_1$ and the numerator is positive near the origin (i.e., $\alpha(V(x)) + L_f V(x) > 0$ on a punctured neighborhood): $q_1 - q_2 < 0$ and $\lim_{v \rightarrow 0} \theta_{\min}(\alpha; v) = \infty$, e.g., scalar system $\dot{x} = x^q u$ with a CLF $V = \frac{1}{2}x^2$, if $q > 1$, any linear comparison leads to infinite actuation level near the origin. If the numerator becomes nonpositive sufficiently close to the origin, the positive part yields 0 instead.

Examples. (i) *Linear comparison* $\alpha(V) = \sigma V$ gives $q_1 = 2$. If $\|L_g V(x)\|_1 \geq c_g \|x\|$ ($q_2 = 1$, e.g., constant g with full actuation and quadratic $V = x^\top P x$), then $\theta_{\min}(\alpha; v) \rightarrow 0$ as $v \rightarrow 0$. (ii) *Root-type* $\alpha(V) = C V^p$ with $p \in (0, 1)$ has $q_1 = 2p$. If $q_2 = 1$, finiteness near the origin requires $2p \geq 1$ (i.e., $p \geq \frac{1}{2}$); for $p < \frac{1}{2}$ the level blows up, reflecting the stiffness of non-Lipschitz rates at the origin.

Proposition 3 (Scaling law: θ_{\min} vs. $\xi\alpha$): Consider $v > 0$ and $\alpha \in \mathcal{K}$, and assume $\theta_{\min}(\alpha; v) < \infty$. For $\xi \geq 0$, define

$$\theta_{\min}(\xi\alpha; v) = \sup_{x \in \Omega(V, v)} \left[\frac{\xi\alpha(V(x)) + L_f V(x)}{\|L_g V(x)\|_1} \right]_+.$$

Then for any $0 \leq \xi_1 < \xi_2 < \infty$,

$$\theta_{\min}(\xi_1\alpha; v) \leq \theta_{\min}(\xi_2\alpha; v).$$

Moreover, if $\theta_{\min}(\xi_1\alpha; v) > 0$, then

$$\theta_{\min}(\xi_2\alpha; v) > \theta_{\min}(\xi_1\alpha; v).$$

Equivalently, if $\theta_{\min}(\alpha; v) > 0$, scaling down ($0 < \xi < 1$) strictly decreases the level, while scaling up ($\xi > 1$) strictly increases it.

Proof: For each $x \in \Omega(V, v)$, let

$$\psi_x(\xi) \doteq \left[\frac{\xi\alpha(V(x)) + L_f V(x)}{\|L_g V(x)\|_1} \right]_+.$$

If $\|L_g V(x)\|_1 > 0$, then $\psi_x(\xi)$ is the positive part of an affine function in ξ with slope $\alpha(V(x))/\|L_g V(x)\|_1 \geq 0$, hence it is nondecreasing (indeed convex). If $\|L_g V(x)\|_1 = 0$, finiteness of $\theta_{\min}(\alpha; v)$ forces the numerator ≤ 0 , so $\psi_x \equiv 0$, which is also nondecreasing. Thus $\theta_{\min}(\xi\alpha; v) = \sup_{x \in \Omega(V, v)} \psi_x(\xi)$ is nondecreasing in ξ , proving $\theta_{\min}(\xi_1\alpha; v) \leq \theta_{\min}(\xi_2\alpha; v)$ for $\xi_2 > \xi_1$. If $\theta_{\min}(\xi_1\alpha; v) > 0$, there exists x^* with $\psi_{x^*}(\xi_1) > 0$. Then necessarily $\alpha(V(x^*)) > 0$ and $\|L_g V(x^*)\|_1 > 0$, so ψ_{x^*} has strictly positive slope at ξ_1 . Hence $\psi_{x^*}(\xi_2) > \psi_{x^*}(\xi_1)$ for any $\xi_2 > \xi_1$, yielding $\theta_{\min}(\xi_2\alpha; v) > \theta_{\min}(\xi_1\alpha; v)$. ■

Therefore, under the linear comparison $\alpha(V) = \sigma V$, the required actuation level is nondecreasing in σ . In fact, if $\theta_{\min}(\sigma_1 V; c) > 0$ and $\sigma_2 > \sigma_1$, then

$$\theta_{\min}(\sigma_2 V; c) > \theta_{\min}(\sigma_1 V; c),$$

so achieving a larger certified exponential rate necessarily requires a greater actuation level (larger $\|u\|_\infty$).

2) **Endpoint-dominated lower bounds (level-wise growth):** To capture how the required input grows with the Lyapunov level, note that for $x \in \Omega(V, v)$, by Assumption 1,

$$\|f(x)\| \leq L_1 \|x\|, \quad \|\nabla V(x)\| \leq L_2 \|x\|, \quad \|g_i(x)\| \leq \bar{g}_i,$$

and the CLF bounds $k_1 \|x\|^2 \leq V(x)$, we have

$$L_f V(x) \leq L_1 L_2 \|x\|^2 \leq \frac{L_1 L_2}{k_1} V \doteq k_3 V, \quad \text{and}$$

$$\begin{aligned} \|L_g V(x)\|_1 &= \sum_i |\nabla V^\top g_i| \leq \|\nabla V\| \sum_i \|g_i\| \\ &\leq L_2 \left(\sum_{i=1}^m \bar{g}_i \right) \|x\| \leq \frac{L_2}{\sqrt{k_1}} \left(\sum_{i=1}^m \bar{g}_i \right) \sqrt{V} \doteq k_4 \sqrt{V}. \end{aligned}$$

Therefore, we obtain a level-wise lower bound:

$$\theta_{\min}(\alpha; v) \geq \sup_{0 < V \leq v} \left[\frac{\alpha(V) - k_3 V}{k_4 \sqrt{V}} \right]_+ \doteq \underline{\theta}_{\min}(\alpha; v). \quad (27)$$

Using $\theta \geq \underline{\theta}_{\min}(\alpha; v)$, (27) gives the necessary level-wise condition (cf. (19))

$$\alpha(V) \leq \bar{\alpha}(\theta, V) \leq k_3 V + \theta k_4 \sqrt{V} \quad (28)$$

Proposition 4 (Endpoint-dominated lower bound): For $\alpha \in \mathcal{K}_l$, $\underline{\theta}_{\min}(\alpha; v)$ is endpoint-dominated that

$$0 < V \leq v, \quad \underline{\theta}_{\min}(\alpha; v) = \left[\frac{\alpha(v) - k_3 v}{k_4 \sqrt{v}} \right]_+.$$

Proof: Write $\alpha(V) = \sigma V$. If $\sigma \leq k_3$, then $\underline{\theta}_{\min}(\alpha; v) \equiv 0$ such that (29) holds. If $\sigma > k_3$, for $V \in (0, v]$, function

$$\frac{\alpha(V) - k_3 V}{k_4 \sqrt{V}} = \frac{\sigma - k_3}{k_4} \sqrt{V}$$

is strictly increasing such that the maximum value is obtained at $V = v$. ■

Both Propositions 3 and 4 show that, for the linear comparison, lowering the endpoint value $\alpha(c)$ is necessary to reduce the actuation level θ_{\min} on $x \in \Omega(V, c)$ (to lower $\|u\|_\infty$).

Proposition 5 (Actuation savings via endpoint relaxation): Consider a window $[\epsilon, c]$ and target rate $\sigma > k_3$. Let the linear baseline be $\alpha_l(V) = \sigma V$ and $\alpha_d(V) = s(V)\sigma V \in \mathcal{K}$ satisfy $\sigma_{\alpha_d}(\epsilon, c) > \sigma$.

(i) *Necessity of endpoint relaxation and concavity:*

$$\underline{\theta}_{\min}(\alpha_d; c) < \underline{\theta}_{\min}(\alpha_l; c) \implies s(c) < 1 (\alpha_d(c) < \alpha_l(c)).$$

Moreover, α_d must be *strictly concave* on a nontrivial subinterval $\mathcal{I}_{\text{cave}} \subset (0, c)$.

(ii) *No savings with linear or convex shapes.* If $\sigma_{\alpha_d}(\epsilon, c) > \sigma$,

$$\forall \alpha_d \in \{\mathcal{K}_l, \mathcal{K}_{\text{vex}}\}, \quad \underline{\theta}_{\min}(\alpha_d; c) > \underline{\theta}_{\min}(\alpha_l; c).$$

Proof: (i) Let $\varphi(\alpha; v) \doteq ([\alpha(v) - k_3 v]_+)/(\theta k_4 \sqrt{v})$. As defined in (27), $\underline{\theta}_{\min}(\alpha; c) \geq \varphi(\alpha; c)$. Since $\underline{\theta}_{\min}(\alpha_l; c)$ is endpoint-dominated, then $\underline{\theta}_{\min}(\alpha_d; c) < \varphi(\alpha_l; c)$ such that $\varphi(\alpha_d; c) < \varphi(\alpha_l; c)$ which implies $\alpha_d(c) < \alpha_l(c)$, i.e., $s(c) < 1$. Due to $\sigma_{\alpha_d}(\epsilon, c) > \sigma$ but $\alpha_d(c) < \sigma c$, then α_d must lie strictly above its chord somewhere on (ϵ, c) by Lemma 3; hence it is strictly concave on a nontrivial subset. (ii) If α_d

is linear with slope $\tilde{\sigma} > \sigma$, then $\alpha_d(c) = \tilde{\sigma}c > \sigma c$ such that $\underline{\theta}_{\min}(\alpha_d; c) > \underline{\theta}_{\min}(\alpha_d; c)$. If α_d is strictly convex and $\sigma_{\alpha_d}(\epsilon, c) > \sigma$, then $\alpha_d(c) > \sigma c$ by Proposition 1, such that the actuation increases. \blacksquare

Consequently, strict concavity is necessary to simultaneously lower θ_{\min} and increase the guaranteed nominal decay rate over the linear baseline.

B. Feasibility-Preserving Acceleration

In this subsection, considering a fixed θ , we show that if a linear baseline is feasible on \mathbb{X} , then any strict margin on a sublevel set can be converted into a *concave* comparison function that (i) remains feasible on \mathbb{X} , and (ii) strictly improves the nominal exponential rate on the evaluation interval $[\epsilon, c]$ contained in that sublevel set.

Theorem 2 (Feasibility-preserving acceleration): Let V be a smooth CLF on \mathbb{X} . Suppose the linear baseline, $\forall x \in \mathbb{X}$,

$$\exists u \in \mathbb{U}(\theta), L_f V(x) + L_g V(x)u \leq -\sigma V(x), \quad (30a)$$

holds for some $\sigma > 0$. Assume there exist $c_0 \in (0, c_{\max}]$ and $\sigma_0 > 0$ such that for all $x \in \Omega(V, c_0)$,

$$\exists u \in \mathbb{U}(\theta), L_f V(x) + L_g V(x)u \leq -(\sigma + \sigma_0)V(x) \quad (30b)$$

Then there exists $\alpha_{\text{cave}} \in \mathcal{K}_{\text{cave}}$ such that $\forall x \in \mathbb{X}$,

$$\exists u \in \mathbb{U}(\theta), L_f V(x) + L_g V(x)u \leq -\alpha_{\text{cave}}(V(x)), \quad (30c)$$

and for every $c \in (0, c_{\max}]$ there exists $\epsilon_0 \in (0, \min\{c, c_0\})$ such that for all $\epsilon \in (0, \epsilon_0)$,

$$\sigma_{\alpha_{\text{cave}}}(\epsilon, c) > \sigma. \quad (30d)$$

Proof: (i) Feasibility: Pick a *concave factor* $s : [0, \infty) \rightarrow (0, \infty)$, strictly decreasing, and satisfies

$$s(0) = (1 + \frac{\sigma_0}{\sigma}), \quad s(c_0) = 1$$

Define $\alpha_{\text{cave}}(v) \doteq s(v)\sigma v$. Then $\alpha_{\text{cave}} \in \mathcal{K}_{\text{cave}}$, $\alpha_{\text{cave}}(v) \leq (\sigma + \sigma_0)v$ for $v \in (0, c_0]$ and $\alpha_{\text{cave}}(v) \leq \sigma v$ $v \in (c_0, c_{\max}]$. Thus (30c) holds. (ii) Acceleration: If $c < c_0$, $s(v) > 1$ holds for $v \in [\epsilon, c]$ with any $\epsilon < c$. Thus, in this case $\sigma_{\alpha_{\text{cave}}}(\epsilon, c) > \sigma$ for any $[\epsilon, c] \subset (0, c_0]$. If $c > c_0$, we have $\sigma_{\text{cave}}(\epsilon, c_0) > \sigma$ and $\sigma_{\text{cave}}(c_0, c) < \sigma$. By Lemma 5, we obtain there always exists a sufficiently small $\epsilon_0 \in (0, c]$ such that for all $\epsilon \in (0, \epsilon_0)$, $\sigma_{\alpha_{\text{cave}}}(\epsilon, c) \in (\sigma, \sigma + \sigma_0)$. \blacksquare

Corollary 1 (Uniform improvement on an interval): Let $c \in (0, c_0]$ and $s : \mathbb{R}_{\geq 0} \rightarrow \mathbb{R}_{>0}$ be a concave factor normalized by $s(c) = 1$ and $s(0) = 1 + \sigma_0/\sigma$ (hence $s(v) > 1$ for all $v \in (0, c)$). Define $\alpha_{\text{cave}}(v) = s(v)\sigma v$ and let $\alpha_l(v) = \sigma v$. Then, for every $\epsilon \in (0, c)$, $\sigma_{\alpha_{\text{cave}}}(\epsilon, c) > \sigma$.

C. Example on the saturated single integrator

Consider $\dot{x} = u$ with $\|u\|_{\infty} \leq \theta$ and the CLF $V(x) = x^2$. Since $L_f V \equiv 0$ and $L_g V = 2x$, by definition

$$D_{\max}(x, \theta) = \bar{\alpha}(\theta, V) = 2\theta\sqrt{V}.$$

Then the (best) global exponential rate $\sigma^* = 2\theta/\sqrt{c}$ for $0 < V \leq c$. The required actuation level for a linear comparison

$\alpha_l(V) = \sigma V$ is $\theta_{\min}(\alpha_l; c) = \underline{\theta}_{\min}(\alpha_l, c) = \sigma\sqrt{c}/2$. With a bang-bang law $u = -\theta \operatorname{sgn}(x)$,

$$\dot{V} = 2xu = -2\theta|x| = -2\theta\sqrt{V} = -\bar{\alpha}(\theta, V),$$

so the windowed nominal rate on $[\epsilon, c]$ is

$$\sigma_{\bar{\alpha}}(\epsilon, c) = \frac{\ln(c/\epsilon)}{\int_{\epsilon}^c \frac{dV}{2\theta\sqrt{V}}} = \frac{2\theta \ln(\sqrt{c}/\sqrt{\epsilon})}{\sqrt{c} - \sqrt{\epsilon}}.$$

Numerical preview $[\epsilon, c] = [10^{-4}, 100]$: Here $\sigma^* = 0.2\theta$ while $\sigma_{\bar{\alpha}}(\epsilon, c) \approx 1.382\theta$, i.e., about 6.9 times faster than the best linear rate with the same θ . The endpoint-relaxation ratio

$$r_{\bar{\alpha}}(\epsilon, c) = \frac{\bar{\alpha}(\theta, c)}{\sigma_{\bar{\alpha}}(\epsilon, c)c} \approx 0.145,$$

quantifies the reduction in endpoint value and, on this window, matches the required–actuation ratio at equal nominal rate (about 85.5% savings).

On trade-offs of non-Lipschitz concave comparison: The bang–bang law (similar to a first–order sliding controller [22]) is discontinuous at $x = 0$ and prone to chattering. In sampled implementations, an insufficient sampling period can aggravate this: even when the comparison function is Lipschitz in V , too large an effective slope can excite high–frequency switching. To retain the decay advantages of concavity while avoiding chattering, the next section introduces a *Lipschitz-aware concave factor* $s(\cdot)$ shaping $\alpha(V) = s(V)\sigma V$ with an explicit slope bound, chosen to match the sampling period and actuator bandwidth. With the rational factor in (31), one has

$$0 \leq s_{\text{rat}}(V) + V s'_{\text{rat}}(V) \leq k_{\max} \implies \left| \frac{d}{dV} \alpha(V) \right| \leq \sigma k_{\max},$$

so k_{\max} directly limits the effective slope.

V. CONSTRUCTIVE CONCAVE FACTORS

The design variable in Theorem 2 is the *concave factor* $s(\cdot)$. In practice (simulation or sampled control), overly fast decay laws can cause chattering or numerical oscillations when the sampling period is not small enough [23]. To address this, we use *Lipschitz-aware* concave factors whose slope can be explicitly capped. A convenient C^{∞} family on $(0, \infty)$ is *rational* form

$$s_{\text{rat}}(v) = \frac{k_{\min}v + k_{\max}\ell}{v + \ell}, \quad 0 \leq k_{\min} < k_{\max}, \quad \ell > 0, \quad (31)$$

which satisfies $s_{\text{rat}}(0) = k_{\max}$, $s_{\text{rat}}(\infty) = k_{\min}$, and

$$s'_{\text{rat}}(v) = -\frac{(k_{\max} - k_{\min})\ell}{(v + \ell)^2}, \quad s''_{\text{rat}}(v) = \frac{2(k_{\max} - k_{\min})\ell}{(v + \ell)^3}$$

We can design a concave comparison function by multiplying a linear comparison with a concave factor.

Lemma 4 (Concavification via a rational factor): For any $\alpha_l(v) = \sigma v \in \mathcal{K}_l$ with $\sigma > 0$, the product

$$\alpha(v) \doteq s_{\text{rat}}(v)\alpha_l(v) = s_{\text{rat}}(v)\sigma v$$

belongs to $\mathcal{K}_{\text{cave}}$ and is locally Lipschitz on $[0, \infty)$.

Proof: Let $F(v) \doteq v s_{\text{rat}}(v) = \frac{k_{\min}v^2 + k_{\max}\ell v}{v + \ell}$. A direct differentiation yields $F'(v) > 0$ and $F''(v) < 0$ implying concavity. Multiplying by the positive constant σ preserves

strict concavity. Local Lipschitzness follows from $|F(v_1) - F(v_2)| \leq k_{\max}|v_1 - v_2|$. \blacksquare

Corollary 2 (Composition of rational factors): For $p \in (0, 1)$, the composed factor $\tilde{s}(v) \doteq s_{\text{rat}}(v^p)$ is again a concave factor in the sense that $\tilde{F}(v) \doteq \tilde{s}(v)v = s_{\text{rat}}(v^p)v$ is strictly concave on $(0, \infty)$.

Proof: Hint: By differentiation, we have $\tilde{F}'(v) > 0, \tilde{F}''(v) < 0$. \blacksquare

This shows that composing the rational factor with a sub-linear power $v \mapsto v^p$ ($p \in (0, 1)$) preserves the ‘‘concave factor’’ property (i.e., $v \mapsto s(v^p)v$ stays strictly concave). It’s a useful strengthening of the rational family since it adds an extra shape parameter p to steepen the near-origin gain while relaxing upper endpoint tuning.

A. Concave–shape tuning

We start from a linear baseline $\alpha_l(v) = \sigma v$, where σ is the best (global) exponential rate available on \mathbb{X} . Consider an evaluation window $[\epsilon, c]$ and design a rational concave factor

$$s_{\text{rat}}(v) = \frac{k_{\min}v + k_{\max}\ell}{v + \ell}, \quad 0 < k_{\min} < 1 < k_{\max}, \quad \ell > 0,$$

so that the concave comparison $\alpha(v) \doteq s_{\text{rat}}(v)\sigma v$ meets performance and feasibility goals on $[\epsilon, c]$. The target nominal rate $\sigma^* > \sigma$ such that $\sigma_{\alpha}(\epsilon, c) \geq \sigma^*$.

1) *Endpoint normalization:* We set $c = V(x_0)$ and impose $s_{\text{rat}}(c) = r \leq 1$ so the endpoint matches the baseline:

$$s_{\text{rat}}(c) = r \iff \ell = \frac{(r - k_{\min})c}{k_{\max} - r}. \quad (32)$$

This leaves two free shape parameters (k_{\min}, k_{\max}) with $k_{\min} \in (0, 1), k_{\max} > 0$.

2) *Exact nominal rate under s_{rat} :* The guaranteed crossing time by α is

$$\begin{aligned} T_{\alpha}(\epsilon, c) &= \frac{1}{\sigma} \int_{\epsilon}^c \frac{y + \ell}{y(k_{\min}y + k_{\max}\ell)} dy \\ &= \frac{1}{\sigma} \left[\frac{1}{k_{\max}} \ln \frac{c}{\epsilon} + \frac{k_{\max} - k_{\min}}{k_{\max}k_{\min}} \ln \frac{k_{\min}c + k_{\max}\ell}{k_{\min}\epsilon + k_{\max}\ell} \right] \end{aligned}$$

Hence, the closed form rate (cf. (12)) is

$$\sigma_{\alpha}(\epsilon, c) = \frac{\sigma k_{\max} \ln(c/\epsilon)}{\ln(c/\epsilon) + \frac{k_{\max} - k_{\min}}{k_{\min}} \ln \frac{k_{\min}c + k_{\max}\ell}{k_{\min}\epsilon + k_{\max}\ell}} > \sigma^*. \quad (33)$$

By (33), we can select a low $k_{\min} < 1$ and solve k_{\max} , or select a sufficiently high $k_{\max} > \sigma^*/\sigma$ and solve k_{\min} .

3) *Feasibility check (necessity):* The sufficient condition of feasibility is that $\alpha(V(x)) \leq D_{\max}(\theta, x)$ along the trajectory $x(t)$. However, the trajectory $x(t)$ is usually not available ahead. The level-wise cap bound presented in (19)

$$\alpha(v) \leq \bar{\alpha}(\theta, v) \leq k_3 v + k_4 \theta \sqrt{v}, \quad \forall v \in (0, c_{\max}].$$

provides a necessary condition, offering a good estimate. Thus, choose $s_{\text{rat}}(\epsilon) < \frac{k_3}{\sigma} + \frac{k_3 \theta}{\sqrt{\epsilon}}$. Combined with (32), this yields an explicit admissible region for (k_{\min}, k_{\max}) with $s(c) = r$.

Practical tuning recipe:

- 1) Choose $[\epsilon, c]$ and target nominal rate σ^* and baseline σ .
- 2) Pick a sufficiently low $k_{\min} \in [0, 1)$ for keeping feasibility. Pick an aggressive $k_{\max} > \sigma^*/\sigma > 1$.
- 3) Enforce $s_{\text{rat}}(c) = r \leq 1$ via (32) to get ℓ .
- 4) Verify $\sigma_{\alpha}(\epsilon, c) \geq \sigma^*$. If not, increase k_{\max}, r and decrease k_{\min} .
- 5) Verify feasibility using the caps $D_{\max}(x, \theta), \bar{\alpha}(\theta, v)$ if available. If not, directly tune based on simulation.
- 6) If feasibility fails (input is saturated), decrease r for relaxing constraint in high-level set and k_{\max} in low-level set.
- 7) If needed, according to the result of Corollary 2, use $s_{\text{rat}}(v^p)$, e.g., $p = 0.5$.

VI. CLF–QP WITH CONCAVE COMPARISON

We integrate the concave comparison framework into a standard CLF–QP pipeline in which the Lyapunov decay rate is designed directly. The key idea is to replace the linear comparison $\dot{V}(x, u) \leq -\sigma V$ with a *concave* constraint

$$\dot{V}(x, u) \leq -s(V(x))\sigma V(x)$$

where $s : \mathbb{R}_{\geq 0} \rightarrow \mathbb{R} > 0$ is a rational concave factor (unless noted, $s(\cdot)$ is the rational concave factor in following contexts), so as to preserve feasibility under actuator limits while strictly increasing the windowed nominal rate $\sigma_{\alpha}(\epsilon, c)$ on a target window $[\epsilon, c]$ (Sec. III).

A. Concave-Shaped CLF–QP

Consider the control-affine system (4) with a smooth CLF V and an input bound $\|u\|_{\infty} \leq \theta$. Given a baseline exponential rate $\sigma > 0$, define

$$\alpha_c(V) \doteq s(V)\sigma V \in \mathcal{K}_{\text{cave}}.$$

The function α_c reshapes the linear baseline while reducing the endpoint value if we impose $s(c) < 1$ at the endpoint $V = c$ in the estimate window (endpoint normalization).

Hard constraint (feasibility required): The CLF–QP with a hard concave comparison constraint is

$$\begin{aligned} \min_u \quad & u^{\top} u \\ \text{s.t.} \quad & L_f V(x) + L_g V(x)u + s(V(x))\sigma V(x) \leq 0, \\ & \|u\|_{\infty} \leq \theta \end{aligned} \quad (34)$$

When $\theta = \infty$, (34) reduces to the *mini-norm* CLF controller (see [19], [24] for the details). When (34) holds for all $x \in \mathbb{X}$, it yields $\dot{V} \leq -\alpha_c(V) = -s(V)\sigma V$ globally. On any window $[\epsilon, c] \subset (0, c_{\max}]$, if $s(c) = 1$, implying $s(v) > 1$ on a subset of $(0, c)$ with positive measure, then

$$T_{\alpha_c}(\epsilon, c) < T_{\alpha_l}(\epsilon, c) \quad \text{and} \quad \sigma_{\alpha_c}(\epsilon, c) > \sigma,$$

i.e., the guaranteed decay strictly improves while keeping the same endpoint. If $s(c) = r < 1$, than we have to tune k_{\min}, k_{\max} to achieve the target using (33).

Soft constraint (always feasible): Introducing a nonnegative slack δ yields the soft CLF–QP:

$$\begin{aligned} \min_{u, \delta} \quad & u^\top H u + q\delta^2 \\ \text{s.t.} \quad & L_f V(x) + L_g V(x)u + s(V(x))\sigma V(x) \leq \delta, \\ & \|u\|_\infty \leq \theta, \quad \delta \geq 0, \end{aligned} \quad (35)$$

with $H \succ 0$ and $q > 0$. This is always feasible; the optimal slack $\delta^*(x)$ induces the closed-loop inequality

$$\dot{V}(x) \leq -s(V(x))\sigma V(x) + \delta^*(x). \quad (36)$$

Proposition 6 (Acceleration for soft CLF–QP): Let $\alpha_l(V) = \sigma V$ and $\alpha_c(V) = s(V)\sigma V$, with normalized rational factor $s(c) = 1$ (hence $s(V) > 1$ on (ϵ, c)). Consider the soft CLF–QP with slack $\delta \geq 0$ as in (35), and assume feasibility on $[\epsilon, c]$. Then the following each imply strict improvement:

- 1) If $\delta^*(x) = 0$ for all states with $V(x) \in [\epsilon, c]$, then $T_{\alpha_c}(\epsilon, c) < T_{\alpha_l}(\epsilon, c)$, equivalently $\sigma_{\alpha_c}(\epsilon, c) > \sigma$.
- 2) If there exists an interval $(a, b) \subset (\epsilon, c)$ such that $\delta^*(x) = 0$ whenever $V(x) \in (a, b)$, then the same strict inequality holds.
- 3) If there exists an interval $(a, b) \subset (\epsilon, c)$ such that $\alpha_c(V) - \delta^*(x) > \alpha_l(V)$ whenever $V(x) \in (a, b)$, then the same strict inequality holds.

Proof: On any interval where the enforced bound satisfies $-\alpha_c(V) + \delta^* < -\alpha_l(V)$, one has $\int_\epsilon^c \frac{dv}{\alpha_c(v) - \delta^*} < \int_\epsilon^c \frac{dv}{\alpha_l(v)}$, yielding $T_{\alpha_c}(\epsilon, c) < T_{\alpha_l}(\epsilon, c)$ and hence $\sigma_{\alpha_c}(\epsilon, c) > \sigma$. ■

Numerical issues induced by slack: With a soft CLF constraint, the optimizer returns a slack $\delta^*(x) \geq 0$ that is rarely *exactly* zero in floating point even when a minimum-norm controller is feasible. The certified instantaneous rate is lower-bounded by

$$\frac{\dot{V}}{V} \geq s(V)\sigma - \frac{\delta^*}{V}.$$

When V is moderate, a small absolute error Δ in the slack (solver tolerance, round-off) has negligible effect: $(\delta^* + \Delta)/V \approx \delta^*/V$. However, as $V \rightarrow 0$, division by V amplifies any residual: even if $\delta^* = 0$, a tolerance-sized perturbation Δ yields $(\delta^* + \Delta)/V = \Delta/V \gg 0$ (e.g., $\Delta = 10^{-4}$ and $V = 10^{-4}$ produce a unit drop in the lower bound). This makes the soft CLF–QP appear significantly more conservative than the minimum-norm (hard) controller near the origin, purely for numerical reasons.

B. Existing CLF–QP frameworks for accelerating decay

Prior CLF–QP approaches accelerate decay primarily by *modulating a global exponential rate* rather than shaping the comparison function. Two representative lines are: (i) hybrid/time–scale scheduling via rapidly exponentially stabilizing CLFs (RES–CLFs) [19]; and (ii) optimization of the rate as a decision variable (“flexible” CLF–QP) [20] and [21].

1) Rapidly exponentially stabilizing CLF–QP: RES–CLF details appear in [19]. The key is a family V_ε with

$$\begin{aligned} c_1 \|x\|^2 \leq V_\varepsilon(x) &\leq \frac{c_2}{\varepsilon^2} \|x\|^2 \\ \inf_{u \in \mathbb{R}^m} \left\{ L_f V_\varepsilon(x) + L_g V_\varepsilon(x) u + \frac{c_3}{\varepsilon} V_\varepsilon(x) \right\} &\leq 0 \end{aligned} \quad (37)$$

where $c_1, c_2, c_3 > 0$ and $\varepsilon \in (0, 1)$. Feasibility yields the decay guarantee

$$\dot{V}_\varepsilon(x) \leq -\frac{c_3}{\varepsilon} V_\varepsilon(x) \doteq -\alpha_\varepsilon(V_\varepsilon(x)),$$

so decreasing ε increases the global exponential rate c_3/ε . Under input constraints $\|u\|_\infty \leq \theta$, however, the maximum exponential rate is capped pointwise by

$$\sigma_{\max}(V) \doteq \bar{\alpha}(\theta, V)/V,$$

which typically decreases with V (e.g., for $\bar{\alpha}(\theta, V) \leq k_3 V + k_4 \theta \sqrt{V}$). Consequently, feasibility at high levels often forces evaluation with a *larger* ε (hence a weaker windowed rate). Any practical acceleration then appears on sublevel sets where the soft constraint is inactive ($\delta^* = 0$). This is consistent with the concave perspective: acceleration arises by reallocating decay away from the endpoint and toward regions with available margin.

2) Flexible CLF–QP: A flexible CLF–QP treats the rate as a decision variable:

$$\min_{u, \sigma} \quad (1 - \kappa(x)) u^\top u + \kappa(x) (\sigma_{\max} - \sigma)^2 \quad (38)$$

$$\text{s.t.} \quad L_f V(x) + L_g V(x) u + \sigma V(x) \leq 0, \quad (39)$$

$$\sigma_{\min} \leq \sigma \leq \sigma_{\max}, \quad \|u\|_\infty \leq \theta, \quad (40)$$

with a locally Lipschitz weight $\kappa : \mathbb{R}^n \rightarrow [\kappa_{\min}, \kappa_{\max}]$, $0 < \kappa_{\min} \leq \kappa_{\max} < 1$. The optimizer selects $\sigma^*(x) \in [\sigma_{\min}, \sigma_{\max}]$; as $\kappa(x) \rightarrow 0$ the problem emphasizes input economy ($\sigma^* \rightarrow \sigma_{\min}$), and as $\kappa(x) \rightarrow 1$ it favors larger rates ($\sigma^* \rightarrow \sigma_{\max}$). With input bounds, the achievable rate is still limited by the endpoint cap via $\sigma^*(x) \leq \sigma_{\max}(V(x))$, which usually decreases with V ; hence global acceleration remains constrained by high-level feasibility.

3) Discussion: Regardless of the CLF–QP variant, under the standing assumptions and for a sufficiently large window $V(x) \in [\epsilon, c]$, actuation demand concentrates at higher levels where $\sigma_{\max}(V)$ is smallest. If we forgo enforcing a *uniform* pointwise rate and instead certify the *windowed nominal rate* $\sigma_\alpha(\epsilon, c)$, then shaping α becomes a powerful degree of freedom. The proposed concave factor $s(V)$ (with controlled slope) dynamically exploits any available slack, preserves feasibility under the same endpoint cap, and provides a computable $\sigma_\alpha(\epsilon, c)$ for offline tuning. If the soft CLF–QP returns $\delta^* = 0$, the target nominal rate is achieved; otherwise, the violation certifies that the target is unattainable under the input constraint.

VII. CASE STUDIES

We present two case studies. The first (an inverted pendulum with torque saturation) is a *toy* yet representative example that walks through the main concepts: (i) actuator–induced caps on Lyapunov decay; (ii) the endpoint–limited baseline exponential rate; and (iii) acceleration via concave comparisons

in a CLF–QP. The second (attitude control for a quadrotor) illustrates that the same design carries over to a practical system subject to tight actuator limits.

A. Common evaluation protocol

For both cases we use a smooth control Lyapunov function (CLF) V and enforce a soft CLF–QP with input bounds:

$$\begin{aligned} \min_{u, \delta \geq 0} \quad & u^\top H u + q \delta^2 \\ \text{s.t.} \quad & L_f V(x) + L_g V(x) u + \alpha(V(x)) \leq \delta, \quad (41) \\ & \|u\|_\infty \leq \theta. \end{aligned}$$

We compare $\alpha \in \{\alpha_l, \alpha_c\}$ where the *linear* baseline is $\alpha_l(V) = \sigma V$ and the *concave* comparison is $\alpha_c(V) = s_{\text{rat}}(V) \sigma V$ with the rational concave factor

$$s_{\text{rat}}(v) = \frac{k_{\min}(v/c) + k_{\max} \ell}{(v/c) + \ell}, \quad 0 < k_{\min} < 1 < k_{\max}.$$

It is normalized at the window endpoint c via $s_{\text{rat}}(c) = r \leq 1$, hence $\ell = (r - k_{\min})/(k_{\max} - r)$ (see (32)). The choice $r = 1$ enforces the *same endpoint* as the linear baseline ($\alpha_c(c) = \alpha_l(c) = \sigma c$); choosing $r < 1$ intentionally relaxes the endpoint to reduce peak actuation. Given an initial condition x_0 , we set $c = V(x_0)$ and $\epsilon = \xi c$ with $\xi \in \{10^{-4}, 10^{-3}, 10^{-2}\}$. The baseline rate σ is taken from the cited reference for each system.

Metrics: We mainly report: (i) the normalized decay $V(x(t))/V(x_0)$; (ii) the exact crossing time $T(\epsilon, c)$ and the induced nominal rate $\sigma_{\text{nom}}(\epsilon, c) \doteq \ln(c/\epsilon)/T(\epsilon, c)$; (iii) the instantaneous exponential rate $-\dot{V}/V$; and (vi) actuation usage $\|u\|_\infty$ and energy $\int_0^{T(\epsilon, c)} u^\top u dt$.

B. Inverted pendulum

We consider a torque–saturated pendulum with viscous friction (as in [25]):

$$\dot{\psi} = \omega, \quad \dot{\omega} = \frac{mgl}{I} \sin \psi - \frac{b}{I} \omega - \frac{1}{I} u, \quad \|u\|_\infty \leq \theta, \quad (42)$$

with $m, l, I, b > 0$, gravity g , state $x = [\psi, \omega]^\top$, and torque bound θ . We adopt a quadratic CLF $V(x) = x^\top P x$ with $P = P^\top \succ 0$ from

$$A_{\text{clf}}^\top P + P A_{\text{clf}} = -\sigma_{\text{clf}} Q_{\text{clf}}, \quad Q_{\text{clf}} \succ 0, \quad \sigma_{\text{clf}} > 0, \quad (43)$$

where

$$A_{\text{clf}} = \begin{bmatrix} 0 & 1 \\ \frac{mgl}{2I} - K_1 & -\frac{b}{I} - K_2 \end{bmatrix}, \quad K_1, K_2 > 0,$$

which encodes a PD template and yields a valid CLF for (42) on a large region around $\psi = 0$ [25].

Parameter settings: Given $x_0 = [\pi/4 \ 0.05]^\top$, set $c = V(x_0)$ and $\epsilon = \xi c$ with $\xi \in \{10^{-4}, 10^{-3}, 10^{-2}\}$. Sampling time $dt = 1 \text{ ms}$. Parameters as in [25]: $(m, l, b, g) = (1, 1, 0.01, 9.81)$, $I = ml^2/3$, $K_1 = 6$, $K_2 = 5$, $\sigma_{\text{clf}} = 3$, $Q_{\text{clf}} = \text{diag}(1, 1)$, $q = 10^5$, $\theta = 10$, baseline $\sigma = 3$ (near the best feasible exponential rate for $\theta = 10$). We set $k_{\max} = 2.3$, $k_{\min} = 0.1$, and $r \in \{1, 0.9, 0.8, 0.7, 0.6\}$. All QPs use quadprog; dynamics are integrated by ode45 with ZOH over each sampling interval.

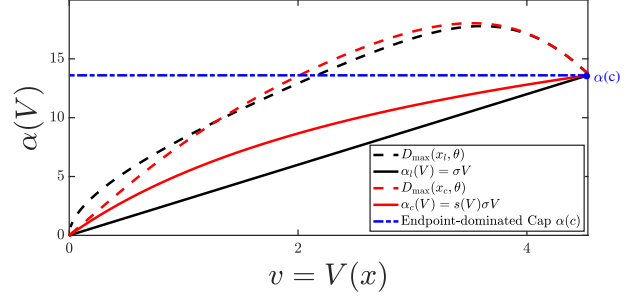


Fig. 2. Assignable decay-rate cap $D_{\text{max}}(x, \theta)$ along the trajectory for $\theta = 10$ and the comparison functions. The endpoint value $\alpha(c)$ strictly restricts the assignable exponential rate.

Results: To expose endpoint domination, we plot the decay rate cap along the trajectory, $D_{\text{max}}(x, \theta)$, overlaid with the candidate comparison functions (Fig. 2): the endpoint value $\alpha(c)$ pins the assignable exponential rate and strictly limits what can be certified. We then simulate the soft CLF–QP for the linear baseline and for concave designs with $s_{\text{rat}}(c) = r$. As shown in Table I, relaxing the endpoint ($r < 1$) reduces the peak actuation $\|u\|_\infty$, confirming the significance of the endpoint cap.

As predicted, with *endpoint normalization* ($r = 1$), the concave design yields a strictly larger windowed nominal rate $\sigma_{\text{nom}}(\epsilon, c)$ (equivalently, shorter $T(\epsilon, c)$) than the linear baseline. For $r \in \{1, 0.9, 0.8, 0.7, 0.6\}$ the controller maintains a large nominal rate while lowering peak actuation (Fig. 3); notably, this acceleration is obtained *without* increasing energy $\int_0^{T(\epsilon, c)} u^\top u dt$.

Finally, with the mini-norm (hard) CLF controller ($\delta \equiv 0$), the instantaneous rate tracks the designed profile $s(V)\sigma$ and remains monotone increasing toward equilibrium, whereas the soft CLF–QP can exhibit small dips at very low V due to the amplification of δ/V (Compare Fig. 4 with Fig. 3).

C. Quadrotor attitude under actuator limits

We consider the quadrotor model of [26], [27]:

$$\dot{x}_p = x_v, \quad (44)$$

$$m \dot{x}_v = m g e_3 - f R e_3, \quad (45)$$

$$\dot{R} = R \hat{\omega}, \quad (46)$$

$$J \dot{\omega} = -\omega \times J \omega + u, \quad (47)$$

where $x_p, x_v \in \mathbb{R}^3$, $m \in \mathbb{R}$, $\omega \in \mathbb{R}^3$, $f \in \mathbb{R}$, $R \in \mathfrak{so}(3)$, $e_3 = [0, 0, 1]^\top$, $J \in \mathbb{R}^{3 \times 3}$, $u \in \mathbb{R}^3$ with $\|u\|_\infty \leq \theta$, and

$$\hat{\omega} = \begin{bmatrix} 0 & -\omega_3 & \omega_2 \\ \omega_3 & 0 & -\omega_1 \\ -\omega_2 & \omega_1 & 0 \end{bmatrix}.$$

We compare the concave CLF–QP with the flexible CLF–QP presented in [20], which is effective for attitude control. We adopt the same CLF from [20]:

$$V(x) = \frac{1}{2} e_\omega^\top J e_\omega + k_R \Psi(R, R_d) + k_c e_R^\top e_\omega,$$

TABLE I
INVERTED PENDULUM: PERFORMANCE METRICS

Controller	$\epsilon_1 = 10^{-2}c$			$\epsilon_2 = 10^{-3}c$			$\epsilon_3 = 10^{-4}c$			$\ u\ _\infty$
	T_{ϵ_1}	σ_{nom}	$\int_0^{T_{\epsilon_1}} u^2 dt$	T_{ϵ_2}	σ_{nom}	$\int_0^{T_{\epsilon_2}} u^2 dt$	T_{ϵ_3}	σ_{nom}	$\int_0^{T_{\epsilon_3}} u^2 dt$	
Linear	1.535	3.000	7.833	1.998	3.000	7.864	3.076	3.000	7.875	9.938
$r = 1.0$	0.860	5.361	7.501	1.196	5.779	7.502	1.535	6.004	7.502	9.938
$r = 0.9$	0.899	5.127	7.337	1.235	5.594	7.338	1.574	5.853	7.338	9.317
$r = 0.8$	0.948	4.858	7.265	1.286	5.377	7.266	1.624	5.673	7.266	8.697
$r = 0.7$	1.013	4.547	7.313	1.351	5.115	7.314	1.690	5.452	7.314	8.078
$r = 0.6$	1.102	4.181	7.530	1.441	4.797	7.531	1.780	5.178	7.531	7.455

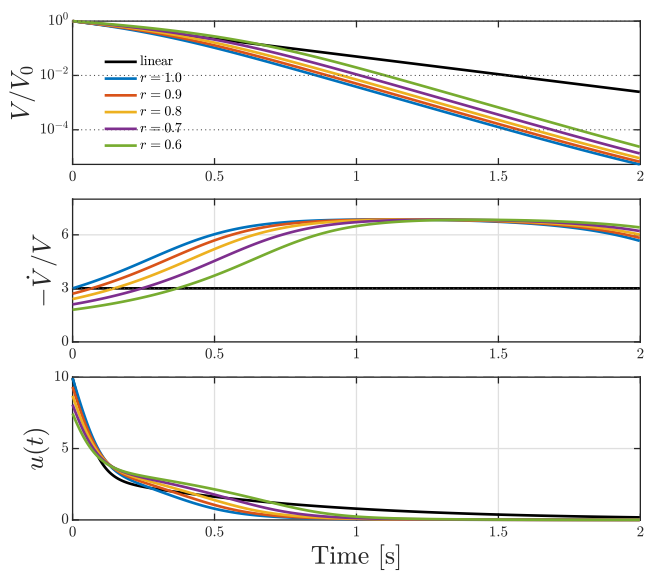


Fig. 3. Inverted pendulum: Normalized Lyapunov response $V(x(t))/V(x_0)$, instantaneous exponential rate $-V/V$, and control input u . For windows with $\epsilon \leq 10^{-1}c$, all concave designs achieve a strictly larger nominal rate than the linear baseline (shorter crossing times). For very small $V \lesssim 10^{-4}c$, the instantaneous rate dip because δ/V grows as $V \rightarrow 0$. In contrast, with the hard (mini-norm) CLF controller ($\delta \equiv 0$), the instantaneous rate remains increasing toward equilibrium, consistent with the slack analysis as shown in Fig. 4.

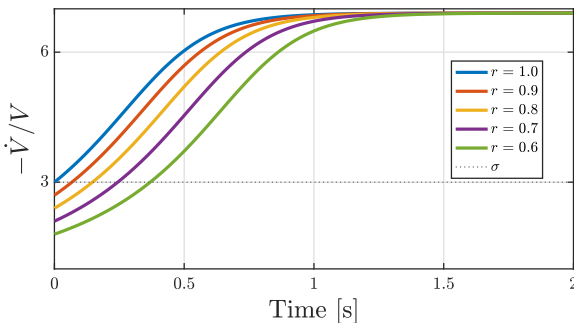


Fig. 4. Inverted pendulum: Mini-norm controllers with concave constraints where the instantaneous rate tracks the designed profiles.

TABLE II
QUADROTOR ATTITUDE: PERFORMANCE METRICS

Controller	$\epsilon_1 = 10^{-2}c$			$\epsilon_2 = 10^{-3}c$			$\ u\ _\infty$
	σ_{nom}	$\int_0^{T_{\epsilon_1}} u^2 dt$	σ_{nom}	$\int_0^{T_{\epsilon_2}} u^2 dt$	σ_{nom}	$\int_0^{T_{\epsilon_2}} u^2 dt$	
Flexible	2.835	0.921	2.827	0.922	10.899	-	
$r = 0.95$	4.523	1.049	3.358	1.050	7.899	-	
$r = 0.85$	4.344	0.785	3.250	0.787	7.068	-	

where $e_\omega = \omega - R^\top R_d \omega_d$, $\Psi(R, R_d) = \frac{1}{2} \text{tr}[I - R_d^\top R]$, and $e_R = \frac{1}{2}(R_d^\top R - R^\top R_d)^\vee$ with the *vee* map $\vee : \mathfrak{so}(3) \rightarrow \mathbb{R}^3$ (see [26], [27]).

Parameter settings.: We focus on attitude control with

$$J = \text{diag}(0.0820, 0.0845, 0.1377) \text{ kg m}^2, \quad m = 4.34 \text{ kg},$$

$$R(0) = \begin{bmatrix} 0.2500 & -0.0580 & 0.9665 \\ 0.4330 & 0.8995 & -0.0580 \\ -0.8660 & 0.4330 & 0.2500 \end{bmatrix}, \quad \omega(0) = 0,$$

$$R_d = I, \quad \omega_d = 0, \quad k_R = 8.81, \quad k_c = 0.1377.$$

All parameters match [20]. For flexible CLF–QP, $\kappa(x) = 0.9(1 - e^{-0.9V(x)})$ and $[\sigma_{\min}, \sigma_{\max}] = [0.29, 10]$ from [20]. For the linear or concave CLF–QP, $H = J^{-1}$ and $q = 300$. The baseline $\sigma = 2$ is chosen to match [20]. We use the normalized rational concave factor with $k_{\min} = 0.8$, $k_{\max} = 2.5$, $r = \{0.85, 0.95\}$ (so $s(c) = r$). Sampling $dt = 1$ ms. Simulations use the Drake Python library. To compare actuation demand, we set $\theta = 11$ to qualify the baseline controller and report the realized $\|u\|_\infty$.

Results: Table II summarizes the windowed nominal rates and energy. Concave CLF–QP gains higher σ_{nom} at comparable or lower energy and *lower peak torque* as shown in Fig. 5.

VIII. CONCLUSION

We showed that shaping α rather than only scaling it is crucial for CLF design under actuator limits. Using the windowed nominal rate $\sigma_\alpha(\epsilon, c)$ and the endpoint cap $\bar{\alpha}(\theta, c)$, strictly *concave* comparisons deliver feasibility-preserving acceleration. A rational, Lipschitz-aware factor yields a practical CLF–QP design with closed-form tuning, and case studies confirm faster guaranteed decay with reduced actuation level and energy. Beyond CLF–QP, the approach *applies to any Lyapunov-based controller* that enforces a comparison inequality (e.g., backstepping, passivity, CCM, LMI). As evidence, our prior passivity-based controller for a 12-D saturated

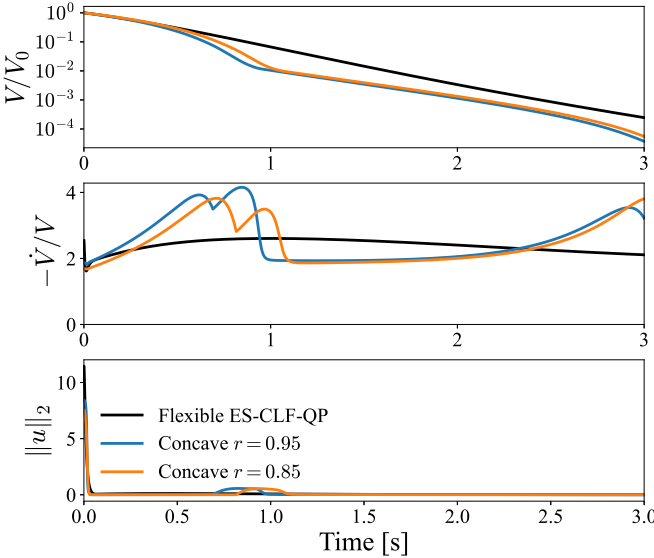


Fig. 5. Quadrotor: normalized Lyapunov response $V(x(t))/V(x_0)$, instantaneous exponential rate $-\dot{V}/V$, and control input norm $\|u\|_2$. The concave CLF-QP yields faster decay than the flexible ES-CLF-QP after $t \approx 0.5$ s; along most of the trajectory, the instantaneous rate exceeds the baseline $\sigma = 2$, consistent with the feasibility-preserving acceleration theorem. With $r = 0.85$, faster decay is achieved with a lower peak input $\|u\|_\infty$ and reduced energy. Decreasing r further reduces the actuation peak, consistent with endpoint-dominated actuation level.

underwater vehicle benefits from concave shaping, improving tracking and robustness [28]. Future work includes CLF/CBF co-design, and sampling-aware and slack-aware slope limits.

REFERENCES

- [1] Y. Lin, E. D. Sontag, and Y. Wang, “A smooth converse lyapunov theorem for robust stability,” *SIAM Journal on Control and Optimization*, vol. 34, no. 1, pp. 124–160, 1996.
- [2] H. K. Khalil and J. W. Grizzle, *Nonlinear systems*. Prentice hall Upper Saddle River, NJ, 2002, vol. 3.
- [3] A. Mironchenko, “Input-to-state stability,” in *Input-to-State Stability: Theory and Applications*. Springer, 2023, pp. 41–115.
- [4] Z. Artstein, “Stabilization with relaxed controls,” *Nonlinear Analysis-Theory Methods & Applications*, vol. 7, no. 11, pp. 1163–1173, 1983.
- [5] E. D. Sontag, “A ‘universal’construction of artstein’s theorem on nonlinear stabilization,” *Systems & control letters*, vol. 13, no. 2, pp. 117–123, 1989.
- [6] S. Bhat and D. Bernstein, “Continuous finite-time stabilization of the translational and rotational double integrators,” *IEEE Transactions on Automatic Control*, vol. 43, no. 5, pp. 678–682, 1998.
- [7] A. Polyakov, “Nonlinear feedback design for fixed-time stabilization of linear control systems,” *IEEE Transactions on Automatic Control*, vol. 57, no. 8, pp. 2106–2110, 2012.
- [8] P. Mestres, A. Allibhoy, and J. Cortés, “Regularity properties of optimization-based controllers,” *European Journal of Control*, vol. 81, p. 101098, 2025.
- [9] A. Levant, “Chattering analysis,” *IEEE Transactions on Automatic Control*, vol. 55, no. 6, pp. 1380–1389, 2010.
- [10] B. Li, S. Wen, Z. Yan, G. Wen, and T. Huang, “A survey on the control lyapunov function and control barrier function for nonlinear-affine control systems,” *IEEE/CAA Journal of Automatica Sinica*, vol. 10, no. 3, pp. 584–602, 2023.
- [11] J. Reher, C. Kann, and A. D. Ames, “An inverse dynamics approach to control lyapunov functions,” in *2020 American Control Conference (ACC)*, 2020, pp. 2444–2451.
- [12] K. Galloway, K. Sreenath, A. D. Ames, and J. W. Grizzle, “Torque saturation in bipedal robotic walking through control lyapunov function-based quadratic programs,” *IEEE Access*, vol. 3, pp. 323–332, 2015.
- [13] A. D. Ames, S. Coogan, M. Egerstedt, G. Notomista, K. Sreenath, and P. Tabuada, “Control barrier functions: Theory and applications,” in *2019 18th European control conference (ECC)*. Ieee, 2019, pp. 3420–3431.
- [14] I. R. Manchester and J.-J. E. Slotine, “Control contraction metrics: Convex and intrinsic criteria for nonlinear feedback design,” *IEEE Transactions on Automatic Control*, vol. 62, no. 6, pp. 3046–3053, 2017.
- [15] M. Chilali and P. Gahinet, “H_{sub} /spl infin// design with pole placement constraints: an lmi approach,” *IEEE Transactions on Automatic Control*, vol. 41, no. 3, pp. 358–367, 1996.
- [16] P. Mhaskar and P. D. Christofides, “Stabilization of nonlinear systems with state and control constraints,” *Automatica*, vol. 41, no. 9, pp. 1521–1531, 2005.
- [17] M. Mahmood and P. Mhaskar, “On constructing constrained control lyapunov functions for linear systems,” in *Proceedings of the 2010 American Control Conference*, 2010, pp. 5191–5196.
- [18] P. Mhaskar and P. D. Christofides, “Robust control of nonlinear systems with bounded uncertainties,” *Systems & Control Letters*, vol. 55, no. 1, pp. 52–61, 2006.
- [19] A. D. Ames, K. Galloway, K. Sreenath, and J. W. Grizzle, “Rapidly exponentially stabilizing control lyapunov functions and hybrid zero dynamics,” *IEEE Transactions on Automatic Control*, vol. 59, no. 4, pp. 876–891, 2014.
- [20] L. Dihel and N.-S. P. Hyun, “Flexible convergence rate for quadratic programming-based control lyapunov functions,” pp. 8845–8851, 2024.
- [21] M. A. Shahrai and L. Lessard, “Spacecraft attitude control under reaction wheel constraints using control lyapunov and control barrier functions,” in *2025 American Control Conference (ACC)*, 2025, pp. 947–952.
- [22] A. Levant, “Quasi-continuous high-order sliding-mode controllers,” *IEEE Transactions on Automatic Control*, vol. 50, no. 11, pp. 1812–1816, 2005.
- [23] V. Acary, B. Brogliato, and Y. V. Orlov, “Chattering-free digital sliding-mode control with state observer and disturbance rejection,” *IEEE Transactions on Automatic Control*, vol. 57, no. 5, pp. 1087–1101, 2012.
- [24] A. D. Ames and M. Powell, “Towards the unification of locomotion and manipulation through control lyapunov functions and quadratic programs,” in *Control of Cyber-Physical Systems: Workshop held at Johns Hopkins University, March 2013*. Springer, 2013, pp. 219–240.
- [25] J. J. Choi, “Cbf-clf-helper 1.0: Library for control barrier function (cbf) and control lyapunov function (clf) based control methods,” 2020. [Online]. Available: <https://github.com/HybridRobotics/CBF-CLF-Helper>
- [26] T. Lee, M. Leok, and N. H. McClamroch, “Geometric tracking control of a quadrotor uav on se (3),” in *49th IEEE conference on decision and control (CDC)*. IEEE, 2010, pp. 5420–5425.
- [27] —, “Control of complex maneuvers for a quadrotor uav using geometric methods on se (3),” *arXiv preprint arXiv:1003.2005*, 2010.
- [28] S. Fan and H. Werner, “Control of underactuated autonomous underwater vehicles with input saturation based on passivity using feedback concavification,” in *2024 European Control Conference (ECC)*. IEEE, 2024, pp. 3233–3238.